

## Self-similar scaling of magnetic energy in the inertial range of solar wind turbulence

J. J. Podesta,<sup>1</sup> D. A. Roberts,<sup>1</sup> and M. L. Goldstein<sup>1</sup>

Received 5 April 2006; revised 31 May 2006; accepted 16 June 2006; published 16 September 2006.

[1] Turbulent magnetic field fluctuations in the solar wind undergo an energy cascade in the inertial range with a characteristic Kolmogorov frequency spectrum  $f^{-5/3}$ . Using magnetic field measurements from the Wind and ACE spacecraft at 1 AU in the ecliptic plane, probability distributions (PDFs) of time-delayed differences of magnetic energy density  $B^2(t)$  are shown to exhibit an approximate self-similar scaling for time lags  $\tau$  in the inertial range of the turbulence, that is, from approximately 10 to 1000 s. The scaling is characterized by a single scaling exponent  $\gamma$ , the Hurst exponent, and a universal PDF that is independent of scale for timescales in the inertial range. It is shown that the scaling exponent and the form of the universal PDF change with the 11-year solar cycle due to the changing nature of the turbulence. The timescale for these changes is roughly estimated to be on the order of 1 or 2 years. Studies of low-order structure functions are performed in an attempt to corroborate the self-similar scaling of the PDFs. It is found that the structure functions do not scale in a self-similar manner indicating that the PDFs are not truly self-similar. Therefore the claimed self-similar scaling of the PDFs is only a rough approximation.

**Citation:** Podesta, J. J., D. A. Roberts, and M. L. Goldstein (2006), Self-similar scaling of magnetic energy in the inertial range of solar wind turbulence, *J. Geophys. Res.*, *111*, A09105, doi:10.1029/2006JA011766.

### 1. Introduction

[2] Approximate self-similar scaling of the magnetic energy density in the solar wind was discovered by *Hnat et al.* [2002] and *Hnat et al.* [2003]. Prior to that, it was well known that the individual components of the magnetic field vector  $\mathbf{B} = (B_x, B_y, B_z)$  do not exhibit self-similar scaling, nor does the magnitude of the magnetic field vector  $B = |\mathbf{B}|$ , but the scaling behavior of quadratic quantities such as  $B^2 = \mathbf{B} \cdot \mathbf{B}$  had not been investigated. The approximate scaling behavior of  $B^2$  is important for studies of solar wind turbulence because it provides a new way to organize and interpret measurements. It also suggests new directions for theoretical modeling that have yet to be explored.

[3] Observations of self-similar scaling in turbulent flows are rare. Self-similar scaling was recently demonstrated in a rapidly rotating turbulent flow in a controlled laboratory experiment [*Baroud et al.*, 2002, 2003; *Baroud and Swinney*, 2003]. Both the probability distribution functions (PDFs) and the structure functions of velocity differences  $v(x + \ell) - v(x)$  were shown to exhibit self-similar scaling with a scaling exponent near 1/2. The value of the scaling exponent differs from the Kolmogorov value 1/3 due to the low Rossby number and the resulting two-dimensional (2-D) nature of the turbulence in this experiment.

[4] In an interesting study of intermittency in the solar wind, *Veltri and Mangeney* [1999] and *Mangeney et al.* [2001] applied wavelet techniques originally developed for studies of atmospheric turbulence to show that if the intermittent events are filtered out of the time series for the velocity and magnetic field components, then the structure functions obtained from the filtered time series, these-called “conditioned structure functions,” exhibit self-similar scaling. For one data record from ISEE and another from the Wind spacecraft which they analyzed they found that the scaling exponents of the conditioned structure functions for the components of the magnetic field and velocity field were close to the Kolmogorov and Kraichnan values 1/3 and 1/4, respectively. The timescales analyzed in these studies cover the range from seconds to days and therefore include the inertial range of the turbulence. The studies by *Hnat et al.* [2002, 2003] are different from those of *Veltri and Mangeney* [1999] and *Mangeney et al.* [2001] in one important respect, namely, that no filtering is performed on the signals prior to analysis of the scaling properties.

[5] The purpose of the study presented here is to employ a large database of in situ solar wind measurements to reassess the scaling behavior of magnetic field fluctuations investigated by *Hnat et al.* [2002]. Large data sets are necessary to obtain good statistics and to resolve the tails of the PDFs. While the rescaled PDFs show a rough agreement, confirming the approximate scaling behavior reported by *Hnat et al.* [2002], a careful analysis of the moments of these distributions indicates that they do not exhibit self-similar scaling. Hence self-similarity of the PDFs is valid only as a rough first approximation and does not hold in a

<sup>1</sup>Laboratory for Solar and Space Physics, NASA Goddard Space Flight Center, Greenbelt, Maryland, USA.

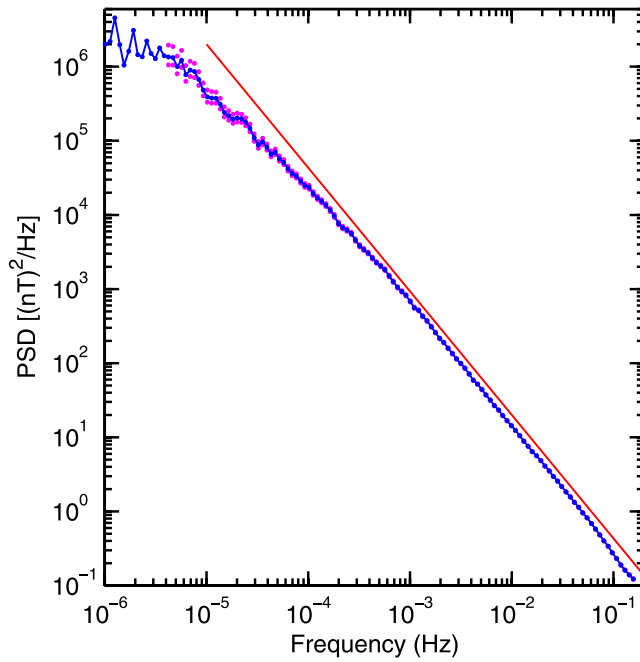


**Figure 1.** Power spectrum of the total magnetic energy given by the sum of the power spectra for  $B_x(t)$ ,  $B_y(t)$ , and  $B_z(t)$ . The component spectra were derived from 3 s Wind MFI data for the time period from 1 November 1997 through 24 June 1998. The 99% confidence interval is a decreasing function of frequency indicated by the magenta markers. The straight red line has a slope of  $-5/3$ .

strict sense. A brief outline of this paper is as follows. The relevant theory is provided in section 2. The procedure and results of the scaling analysis of the PDFs are presented in section 3. Solar cycle effects are studied in section 4. The analysis of the structure functions are described in section 5 and the conclusions are summarized in section 6.

## 2. Self-Similar Processes

[6] If  $B^2(t)$  is the magnetic energy density measured at a point in space, consider the stochastic process

$$x(\tau) = B^2(t + \tau) - B^2(t) \quad (1)$$

which, for fixed  $t$ , is a function of the time delay  $\tau$ . This process is self-similar if there is a constant  $\gamma$  such that the processes  $x(a\tau)$  and  $a^\gamma x(\tau)$  have the same finite dimensional distributions for all  $a > 0$  [Samorodnitsky and Taqqu, 1994; Embrechts and Maejima, 2002]. The constant  $\gamma$  is called the Hurst exponent,  $\gamma > 0$ . If  $x(\tau)$  is self-similar, then it follows from the definition that the first order PDF  $P(x, \tau)$  satisfies the scaling relation

$$P(x, a\tau) = \frac{1}{a^\gamma} P\left(\frac{x}{a^\gamma}, \tau\right). \quad (2)$$

This equation is derived in Appendix A. Hence at the origin  $x = 0$  the probability distribution satisfies the relation

$$P(0, a\tau) = \frac{1}{a^\gamma} P(0, \tau), \quad (3)$$

which implies

$$P(0, \tau) = A\tau^{-\gamma}, \quad (4)$$

where  $A$  is a constant. To derive this result, one may differentiate equation (3) with respect to  $a$  and then set  $a = 1$ .

[7] Equation (2) has the general solution

$$P(x, \tau) = \frac{1}{\tau^\gamma} f\left(\frac{x}{\tau^\gamma}\right), \quad (5)$$

where  $f(x)$  is an arbitrary PDF. To derive this result, one can differentiate equation (2) with respect to  $a$ , set  $a = 1$ , and then find the general integral of the resulting equation using standard methods as described, for example, by Zachmanoglou and Thoe [1986]. Thus if the process  $x(\tau)$  is self-similar, then its PDF obeys the scaling relation (5).

[8] It is well known that for the solar wind, as for other kinds of geophysical and laboratory turbulence, the first order PDFs of velocity differences do not obey a simple scaling relation of the form (5). This is generally attributed to intermittency. However, as indicated in studies by Hnat *et al.* [2003], energy variables such as the magnetic energy density do appear to exhibit self-similar PDFs throughout the inertial range of the turbulence. This important observation is studied further in the following section. A more difficult and as yet unanswered question is whether the stochastic process (1) is approximately self-similar. This depends on the higher order statistics of the non-Gaussian process  $x(\tau)$ .

## 3. Scaling Analysis of Magnetic Energy

[9] Data from the Wind and ACE spacecraft were used to compute PDFs of time delayed differences of the magnetic energy density

$$x(\tau) = B^2(t + \tau) - B^2(t) \quad (6)$$

where  $B^2 = \mathbf{B} \cdot \mathbf{B}$  and  $\mathbf{B}(t)$  is the magnetic field vector measured at the location of the spacecraft. Because the speed of the spacecraft is much smaller than the speed of the solar wind, the change in position of the spacecraft over the time interval  $\tau$  is negligible. The scaling behavior of the PDFs was studied for time delays  $\tau$  in the inertial range of the turbulence. The inertial range can be roughly defined as the frequency range of the power spectrum over which the Kolmogorov spectrum  $f^{-5/3}$  is approximately valid. A sample power spectrum for the total magnetic energy in the solar wind is shown in Figure 1. By inspection of Figure 1, one can see that the inertial range extends from approximately  $10^{-4}$  to  $10^{-1}$  Hz or from 10 to  $10^4$  s.

[10] The scaling behavior of the PDFs is analyzed using the following three-step procedure. Step 1: Compute the empirical PDFs of the quantity  $x(\tau)$  for different values of the time lag  $\tau$ . Step 2: Plot the maximum value of the empirically determined PDFs versus the time lag  $\tau$  on a log-log plot and determine the scaling exponent  $\gamma$  by performing a linear least squares fit (see equation (4)). Step 3: Rescale the PDFs according to the scaling relation (5), that is, plot  $\tau^\gamma P(x, \tau)$  versus  $x/\tau^\gamma$  to see if the rescaled PDFs all lie on a common curve  $f(x)$ .

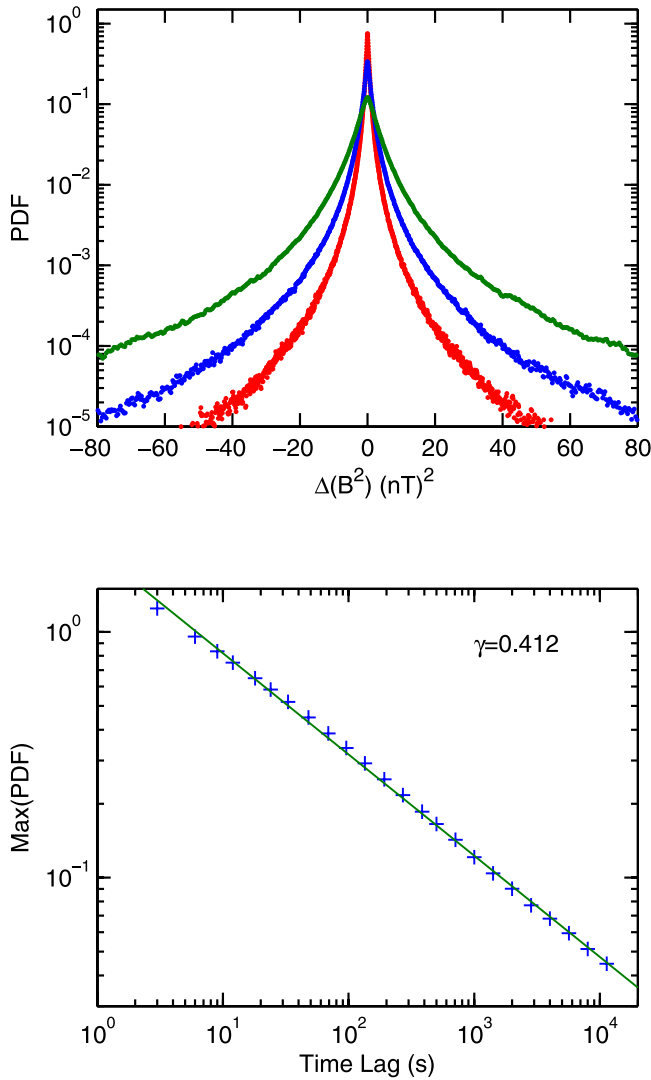


**Figure 2.** (top) PDFs of  $B^2(t + \tau) - B^2(t)$  for  $\tau = 12, 96,$  and  $1000$  s (R/B/G, respectively) obtained from 3 s Wind MFI data for the time period from 28 December 1994 through 1 August 1995. A plot of the maxima of the PDFs versus the time delay  $\tau$  (bottom) yields the scaling exponent  $\gamma = 0.41$ .

[11] The scaling exponent can be computed in different ways. An alternative to the procedure in Step 2 is to plot the absolute moment  $\langle |x(\tau)| \rangle$  versus time lag  $\tau$  on a log-log plot. The slope of the curve then yields an estimate of  $\gamma$ . The results obtained this way are in close agreement with the results obtained from the procedure described in Step 2 in the previous paragraph.

[12] The magnetic field data used in this study consists of 3 s averages from the Wind MFI instrument [Lepping *et al.*, 1995] and 16 s averages obtained from the ACE MAG instrument [Smith *et al.*, 1998]. Whereas ACE is in continuous orbit about the Earth-Sun L1 Lagrangian point, approximately 200  $R_e$  upstream of the Earth's bow shock, Wind follows a maneuverable orbit which sometimes traverses the bow shock and enters the magnetosphere. For Wind, time intervals when the spacecraft was inside the magnetosphere or very near the magnetopause have been

excluded from the data set. This is done using the GSFC list of bow shock crossings compiled by Adam Szabo and the Wind MFI team.

[13] Before the data is analyzed, it is inspected for obvious outliers and unusual behavior. Obvious outliers are identified as single data points or small groups of data points possessing unusually large magnitude and are deleted. The progression of time stamps for the data is also inspected to ensure there are no irregularities such as negative time increments. A few such instances are sometimes found and the associated data is then deleted or corrected. After each of the GSE components  $B_x, B_y,$  and  $B_z$  has been inspected, the magnitude squared  $B^2 = B_x^2 + B_y^2 + B_z^2$  is computed and then saved together with the corresponding timing information. This completes the preprocessing of the data.

[14] To compute the PDF of  $x(\tau)$  at a given time lag  $\tau$ , the differences  $B^2(t) - B^2(t + \tau)$  are first computed by proceeding sequentially through the data list and subtracting pairs of data points having the desired time lag. The resulting sequence of differences  $x_n(\tau)$  are “binned” into subintervals and the number of differences in each bin is counted. An estimate of the PDF at the center of each bin (subinterval) is equal to the bin count divided by the total number of data differences divided by the bin width. By construction, the bin centers are symmetrically located about the center of the distribution. The bin widths are geometrically increasing to better accommodate the decreasing numbers of points in the tails of the distribution. Moreover, the bins all overlap by 50% to provide almost continuous estimates of the PDF.

[15] Figure 2 (top) shows examples of the PDFs computed from Wind MFI data for the period 28 December 1994 0000:00 UT through 1 August 1995 0000:00 UT. This 7 month interval contains  $6.14 \times 10^6$  data points and was chosen because it contains no bow shock crossings. The PDFs shown in Figure 2 (top) indicate that the width of the distribution increases as the time lag  $\tau$  increases. The scaling behavior is investigated by plotting the maximum value of the PDF versus the time lag  $\tau$  as shown in Figure 2 (bottom). The scaling exponent  $\gamma = 0.41$  is obtained by fitting a straight line to  $\log[P(0, \tau)]$  versus  $\log(\tau)$  using linear least squares.

[16] The rescaled PDFs shown in Figure 3 are found to lie approximately on the same curve for time lags  $\tau$  throughout the inertial range. The upper plot is drawn on a linear scale and the lower plot is drawn on a logarithmic scale to show the tails of the distribution. Note that the range of the abscissa in the lower plot in Figure 3 is greater than that in the upper plot by a factor of 25. The rescaled PDFs are in close agreement except for a small discrepancy in the immediate neighborhood of the peak (Figure 3, top). In the tails of the distribution the statistical errors increase as indicated by the scatter of the points in Figure 3, bottom. The agreement between the different PDFs becomes more uncertain for points far out in the tails but is still within the error bars.

[17] The scaling behavior for the squares of the components  $B_x^2, B_y^2,$  and  $B_z^2$  were examined separately using the same procedure used for  $B^2 = B_x^2 + B_y^2 + B_z^2$ . The results in Figure 4 show that the PDFs of the individual components exhibit an approximate scaling behavior with a scaling exponent in each case that is close to the scaling exponent found for  $B^2$  (within 10 percent). The self-similar scaling of the components is only approximate, however, because the rescaled PDFs for different time lags show deviations in the

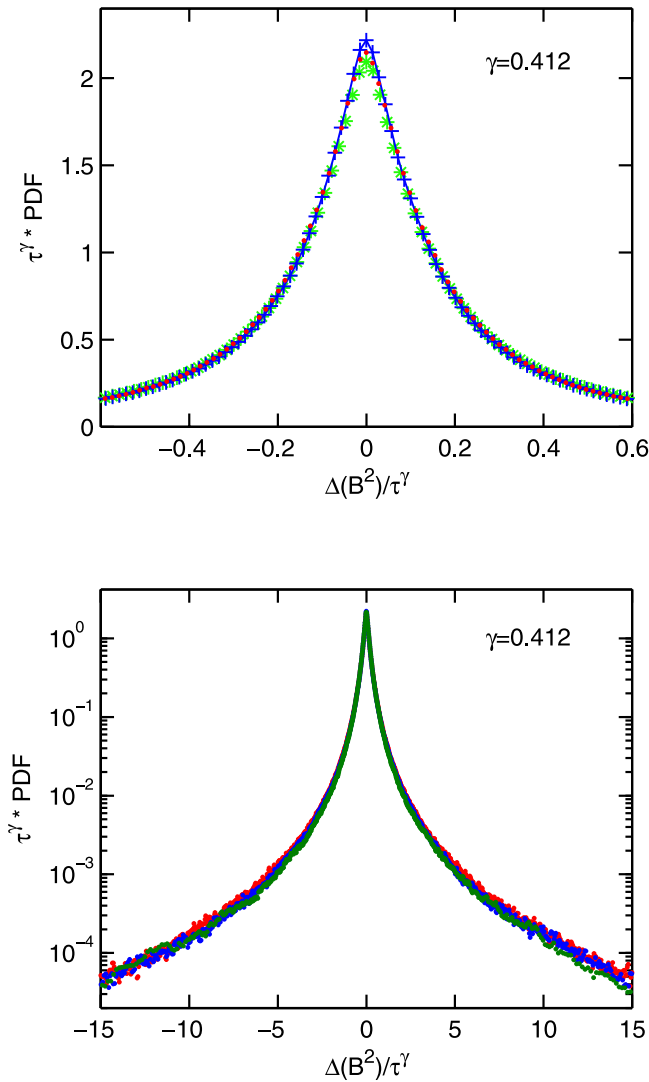


**Figure 3.** The rescaled PDFs corresponding to Figure 2 for time lags  $\tau = 12, 96,$  and  $500$  s given by the symbols in green, blue, and red, respectively (top) and red, blue, and green, respectively (bottom). The upper plot (linear scale) shows the center of the distribution and the lower plot (logarithmic scale) shows the tails of the distribution.

tails. The rescaled PDFs differ by as much as a factor of two in the extreme tails of the distribution. These deviations are not considered to be statistically significant since they are of the same order of magnitude as the error bars estimated from the scatter of the data in Figure 4. To obtain significantly better statistics requires a much larger data set, larger by a factor of ten or more. This is an interesting line of investigation for future research.

[18] Close inspection of the PDFs for the separate components  $B_x^2, B_y^2,$  and  $B_z^2$  show that they are approximately symmetric and that the first derivative is discontinuous at the origin. Analysis of the PDFs with a much finer grid spacing (not shown) reveal that the peak of the distribution forms a cusp. This is in contrast to the PDFs for  $B^2 = B_x^2 + B_y^2 + B_z^2$  that are found to possess a continuous first derivative

at the origin. It is puzzling why the behavior of the PDF of  $B^2$  in the neighborhood of the origin is different from those of  $B_x^2, B_y^2,$  and  $B_z^2$ .

[19] Confirmation of the scaling behavior seen in the MFI data is obtained from the ACE MAG data. The record of ACE MAG 16 s averages from 1 January 1998 through 31 December 2005 contains approximately 16 million data points. Figure 5 (top) shows examples of the PDFs at different scales obtained from this record of ACE MAG data. Note that the width of the PDF increases as the time lag  $\tau$  increases. The scaling behavior in the inertial range of the turbulence is illustrated in Figure 5 (bottom) which yields the scaling exponent  $\gamma = 0.40$ . This is close to the value  $\gamma = 0.41$  obtained independently from Wind MFI data in Figure 2. Both of these values are consistent with the values  $\gamma = 0.43$  and  $\gamma = 0.39$  found in the study by *Hnat et al.* [2003] using Wind data spanning the period from 1995 to 1998.

[20] Using the scaling exponent obtained in Figure 5 (bottom) the PDFs are rescaled according to equation (5). The results for three of the rescaled PDFs are shown in Figure 6. The rescaled PDFs agree remarkably well in the center of the distribution except at the smallest timescales, 16 and 32 s, where the distribution is slightly wider. A reasonably good agreement is also found in the tails of the distribution as shown in Figure 6 (bottom).

#### 4. Is There a Universal PDF?

[21] For time lags  $\tau$  in the inertial range of the turbulence, the scaling procedure reduces the PDFs for different time lags to a single curve  $f(x)$ . In this sense, there is a universal PDF which characterizes the inertial range of the turbulence. What type of PDF is this? The results presented in this study indicate that it has a continuous derivative at the origin and is a member of the class of subexponential distributions, that is, it has “stretched-exponential” tails. The exact mathematical form of this distribution is a fundamental question for future research.

[22] Upon comparing the rescaled PDFs from Wind in Figure 3 and ACE Figure 6 it is immediately apparent that the two PDFs are different. The ACE PDF is wider and, consequently, possesses a smaller peak value than the Wind PDF. Since both sets of measurements were performed at 1 AU using almost identical magnetometers, such a significant difference between the two PDFs was unexpected. Could these differences be caused by solar cycle effects? To answer this question a scaling analysis of the data was performed separately for each year. Because the standard Wind MFI data product has a much higher time resolution than the standard ACE MAG data product, the Wind data was used for this purpose. Because both magnetometers are nearly identical (the ACE magnetometer is the flight spare for Wind) and both spacecraft are exposed to similar solar wind conditions, the results for both magnetometers in any given year should be statistically similar.

[23] Three time intervals were analyzed: 28 December 1994 through 1 August 1995, 1 November 1997 through 24 June 1998, and 1 December 2002 through 7 August 2003. The three intervals analyzed will be referred to briefly as 1995, 1998, and 2003. From plots of the Zurich sunspot number, one can see that these three time intervals occurred

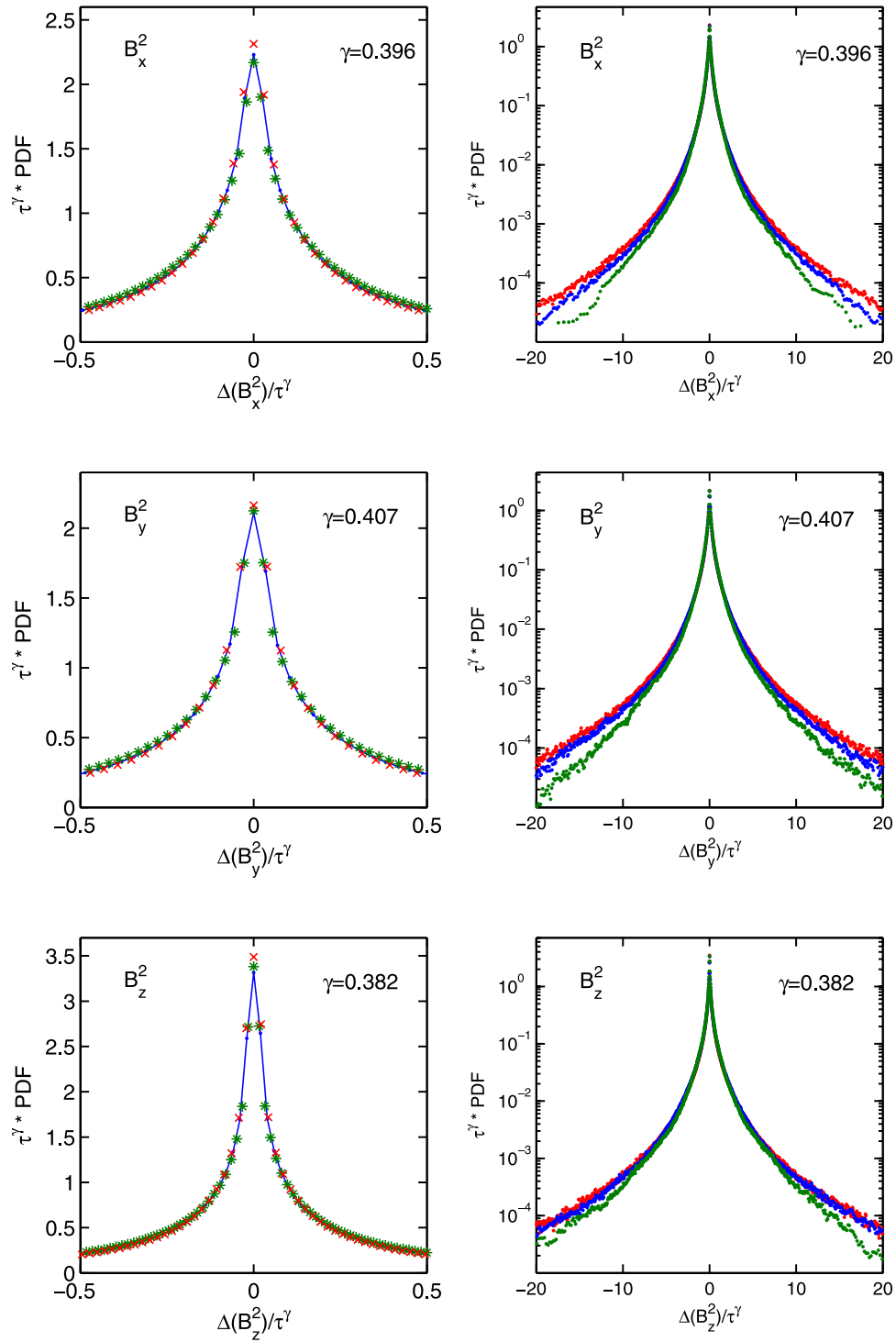


**Figure 4.** Rescaled PDFs for the squared components  $B_x^2$ ,  $B_y^2$ , and  $B_z^2$ , at time lags  $\tau = 12, 96$ , and  $500$  s (red, blue, and green, respectively) obtained from wind MFI data for the time interval 28 December 1994 through 1 August 1995. The plots on the left-hand side are drawn on a linear scale and those on the right-hand side are drawn on a logarithmic scale.

during solar minimum, the rising phase of solar cycle 23, and the declining phase of solar cycle 23, respectively. Each of these three intervals are free from bow shock crossings so that uninterrupted solar wind measurements were performed continuously in each case (except for occasional data gaps).

[24] The rescaled PDFs for 1995, 1998, and 2003 are shown in Figure 7. It is clear from Figure 7 that the scaling behavior and, in particular, the form of the PDF changes during the course of the solar cycle. Note that the PDF for 2003 is much wider than for 1995 or 1998. This indicates a

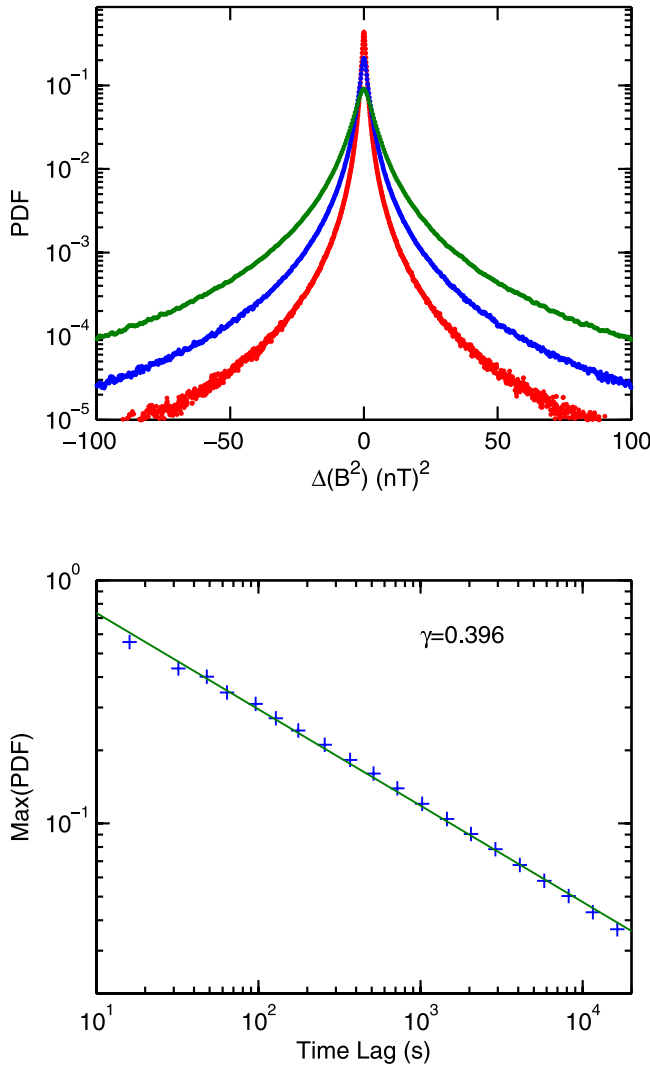


**Figure 5.** (top) PDFs of  $B^2(t + \tau) - B^2(t)$  for  $\tau = 32, 256,$  and  $2048$  s (R/B/G, respectively) obtained from 16 s ACE MAG data for the 8 year period from 1 January 1998 through 31 December 2005. A plot of the maxima of the PDFs versus the time delay  $\tau$  (bottom) yields the scaling exponent  $\gamma = 0.40$ .

larger variance in 2003 and is caused by larger and/or more frequent jumps in the signal  $B^2(t)$ . This is probably associated with the higher frequency of occurrence of CMEs usually observed at solar maximum and during the declining phase of the solar cycle and also the observed occurrence of recurrent high-speed streams in 2003 [Tanskanen *et al.*, 2005]. These conditions are fundamentally different than the quiescent solar wind conditions typical around solar minimum and at the beginning of the rising phase of the cycle.

[25] To answer the question posed at the beginning of this section, it would appear that there does not exist a universal PDF capable of describing the magnetic fluctuations in solar wind turbulence (at 1 AU in the ecliptic plane) because the form of this PDF changes during the eleven year solar cycle. The existence of solar cycle variations rules out the possibility of a unique scaling law and a unique PDF that holds for all time. This is a consequence of the regular changes in

solar wind conditions and the changing characteristics of solar wind turbulence over the course of a typical solar cycle. As a consequence, scaling exponents and PDFs obtained from long time averages, such as the 8 year average of ACE data performed in this study, do not provide an accurate characterization of the turbulence PDF at a particular phase of the solar cycle. In general, the statistical analysis of scaling laws using data records that exceed 1 or 2 years in length are probably affected by solar cycle changes in the underlying turbulence.

## 5. Structure Functions

[26] Another approach that can be used to investigate the scaling of the magnetic energy density is to study the scaling properties of its statistical moments, also called structure functions. For a probability distribution that satisfies the

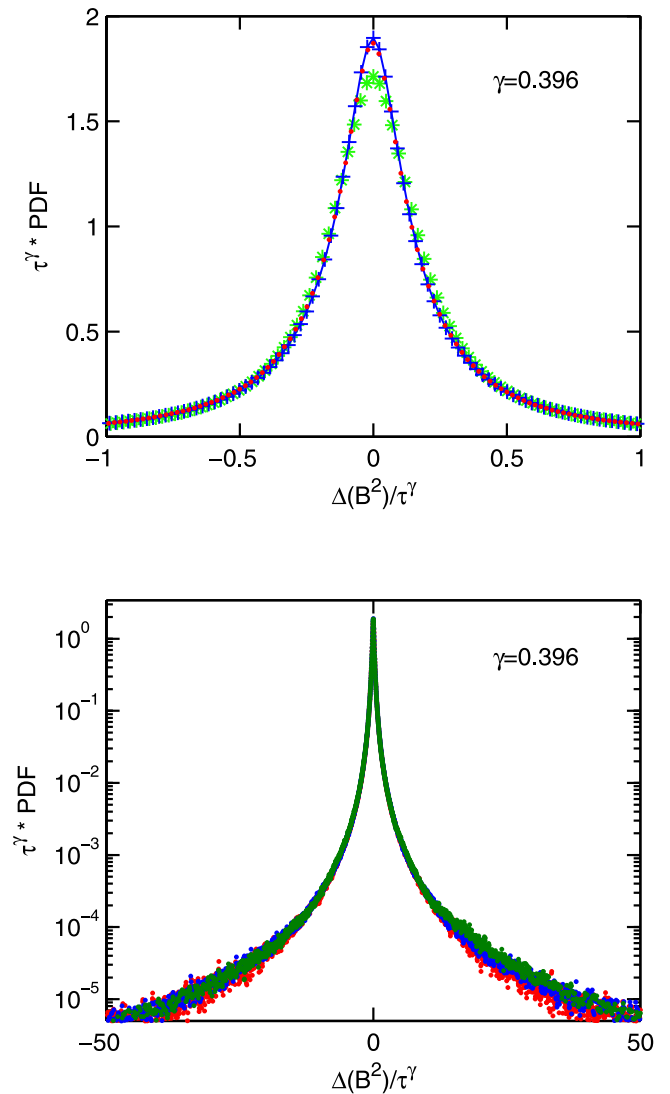


**Figure 6.** The rescaled PDFs corresponding to Figure 5 for time lags  $\tau = 32, 256,$  and  $1456$  s are plotted in green, blue, and red, respectively (top) and red, green, blue, respectively (bottom). The upper plot (linear scale) shows the center of the distribution and the lower plot (logarithmic scale) shows the tails of the distribution.

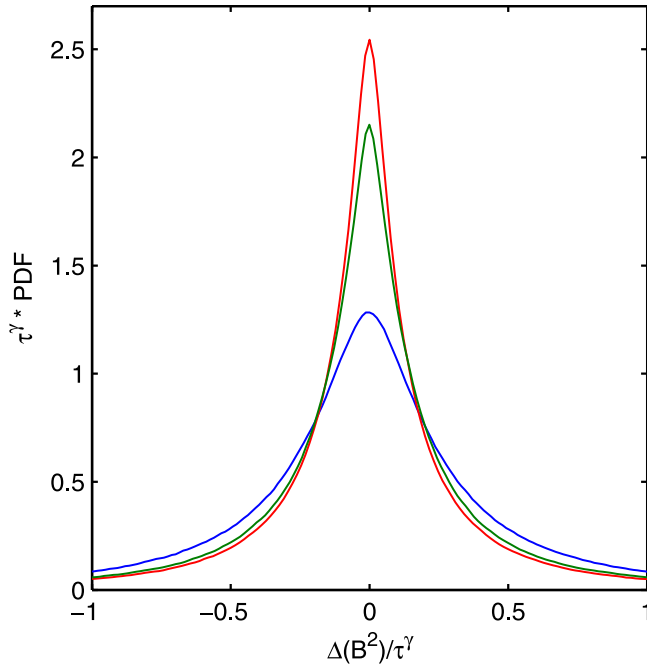


**Figure 7.** The rescaled PDFs from separate analysis of Wind MFI data for the years 1995, 1998, and 2003 are given by the green, red, and blue curves, respectively. The scaling exponents for each year are given by  $\gamma = 0.41, 0.44,$  and  $0.37,$  respectively.

scaling relation (5) the absolute moment of order  $p > 0$  satisfies the scaling relation

$$\langle |x(\tau)|^p \rangle = C_p \tau^{\gamma p}, \quad (7)$$

where  $C_p$  is independent of  $\tau$ . Thus the moment of order  $p$  scales as  $\tau^{\gamma p}$ . The moments are estimated from the data using the formula

$$\langle |x(\tau)|^p \rangle = \frac{1}{N} \sum_{n=1}^N |x_n(\tau)|^p, \quad (8)$$

where  $N$  is the number of data points  $x_n$ . To minimize roundoff error the data sequence  $|x_n(\tau)|^p$  is first sorted in ascending order and then summed starting with the smallest value. The average value of  $x(\tau) = B^2(t + \tau) - B^2(t)$  is close to zero for all of the data studied here.

[27] In general, the accurate estimation of the structure functions (7) requires a large data set. Moreover, the number of data points required to achieve a given accuracy is a rapidly increasing function of  $p$ . The record of 3 s Wind MFI data used in this study, with  $N \simeq 6 \times 10^6$  data points, allows the accurate calculation of the first four moments. This was checked using a random number generator to produce random samples from a “stretched-exponential” distribution  $\exp(-|x|^{1/2})/4$ , a rough approximation to the measured PDFs of  $B^2(t + \tau) - B^2(t)$ . These random samples were then used to estimate the moments for a data set of size  $N = 6 \times 10^6$  and the results were compared with the known exact moments of the stretched-exponential distribution  $(2p + 1)!$ . These Monte Carlo calculations show

that for  $N = 6 \times 10^6$  the estimates of moments from the data is accurate for the first four moments with an error on the order of one percent for  $p = 4$ . It should be noted that these conclusions are independent of the scaling of the PDF so that the same conclusions are obtained for the PDF  $\exp(-|x/a|^{1/2})/4a$  for all  $a > 0$ . The structure functions obtained using 3 s Wind MFI data are shown in Figure 8, top.

[28] Linear least squares fits on a log-log plot yield the power law behavior  $\langle |x(\tau)|^p \rangle \propto \tau^{\xi_p}$  with the exponents  $\xi_p$  shown in the figure. To focus on the inertial range the fit is restricted to timescales less than approximately 180 s, although the overall trends discussed next are independent of the chosen cutoff. The fits obtained show that for the first and second moment the scaling exponents are close to the expected values  $\xi_p = \gamma p$  where  $\gamma = 0.41$  is the scaling exponent determined in section 3. The third and fourth

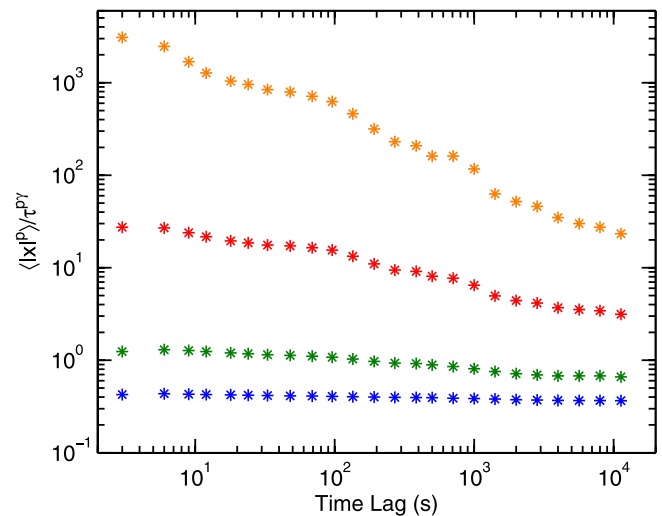
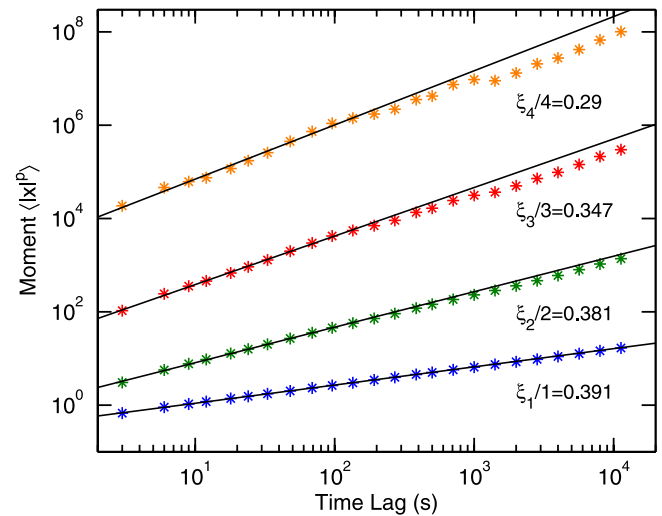


**Figure 8.** The moments (top) and compensated moments (bottom) for  $x(\tau) = B^2(t + \tau) - B^2(t)$  obtained from 3 s Wind MFI data for the time period from 28 December 1994 through 1 August 1995. The scaling exponent derived from the scaling analysis in section 3 is given by  $\gamma = 0.41$ .

moments, however, shows definite deviations from the values predicted by a self-similar scaling of the PDF. The differences between the expected values  $\gamma p$  and the observed values  $\xi_p$  increase monotonically with the parameter  $p$ . These conclusions are corroborated by the lower plot in Figure 8 which shows the ratio  $\langle |x(\tau)|^p \rangle / \tau^{\gamma p}$  where  $\gamma = 0.41$  is the scaling exponent determined in section 3. The structure functions obtained from the other two records of 3 s MFI data, 1998 and 2003, behave in a similar manner.

[29] The analysis of structure functions given in this section indicates that the PDFs of  $B^2(t + \tau) - B^2(t)$  are not self-similar over the range of timescales studied. How is this conclusion to be reconciled with the conclusion in section 3? While the analysis in section 3 shows that the rescaled PDFs lie approximately on the same curve  $f(x)$ , the agreement is not exact. Small deviations between the rescaled PDFs that may not be easily detectable by visual inspection of the plots in section 3 may be responsible for the observed differences in the moments (structure functions). The analysis of structure functions presented in this section implies that self-similar scaling of PDFs found by *Hnat et al.* [2002] and confirmed in section 3 of this paper is only a rough approximation. A mathematically precise self-similar scaling of the PDFs requires that the scaling of the structure functions obey the scaling relation (7). It is possible that more accurate solar wind measurements, including more accurate measurements of the magnetic field variations during rare solar wind events, may eventually lead to the demonstration of self-similar scaling of  $B^2$ , but this would require the agreement between the PDF scaling analysis in section 3 and the structure function analysis in section 5.

## 6. Discussion and Conclusions

[30] The analysis of magnetometer data from the Wind and ACE spacecraft demonstrates the approximate self-similar scaling of PDFs of the magnetic energy density  $B^2(t)$  in the solar wind. This analysis confirms and extends the pioneering studies by *Hnat et al.* [2002] and *Hnat et al.* [2003] by using a larger statistical database. The scaling behavior is characterized by a single scaling exponent  $\gamma$  that is easily extracted from the data. Because the scaling behavior holds for all time lags in the inertial range, the rescaled PDF provides a convenient way to characterize the statistics of solar wind turbulence.

[31] An interesting new result is the observed variation in the scaling exponent  $\gamma$  and the “universal” PDF over the course of the solar magnetic cycle. The analysis shows that variations in  $\gamma$  over the solar cycle are generally small being less than approximately 10%. Such changes are to be expected since many properties of the solar wind, including solar wind fluctuations, are known to vary significantly with the solar cycle.

[32] In addition to studies of the functional form of the rescaled PDFs, attempts to corroborate the scaling of the PDFs were performed by analyzing the scaling behavior of structure functions. The results show that the structure functions of orders 1 through 4 do not scale in a manner consistent with the self-similar scaling of the PDFs. This may be due to small differences between the rescaled PDFs that are not easily detectable by visual inspection of the plots in section 3. Consequently, the self-similar scaling of the PDFs

found by *Hnat et al.* [2002] and confirmed in section 3 of this paper can only be characterized as a rough approximation. In a rigorous mathematical sense, the PDFs are not self-similar. Nevertheless, the rough agreement between the rescaled PDFs should still prove useful as a means of organizing solar wind data.

[33] To continue this research, it is of interest to use much higher resolution magnetometer data, 10 or 20 vectors per second, to improve the statistical studies of self-similar scaling performed here. Such data can also be used to study possible scaling behavior in the dissipation range of the turbulence.

## Appendix A: Derivation of the Scaling Relation

[34] It follows from the definition of  $P(x, \tau)$  that

$$\Pr\{x(\tau) \leq x_0\} = \int_{-\infty}^{x_0} P(x, \tau) dx. \quad (\text{A1})$$

Therefore,

$$\Pr\{x(a\tau) \leq x_0\} = \int_{-\infty}^{x_0} P(x, a\tau) dx \quad (\text{A2})$$

and

$$\Pr\{a^\gamma x(\tau) \leq x_0\} = \int_{-\infty}^{x_0/a^\gamma} P(x, \tau) dx. \quad (\text{A3})$$

By a change of variable, the last equation can be written

$$\Pr\{a^\gamma x(\tau) \leq x_0\} = \frac{1}{a^\gamma} \int_{-\infty}^{x_0} P(x/a^\gamma, \tau) dx. \quad (\text{A4})$$

If the process  $x(\tau)$  is self-similar, then equations (A2) and (A4) must be equal for all  $a > 0$  and for all  $x_0$ . Hence one obtains

$$\int_{-\infty}^{x_0} \left[ P(x, a\tau) - \frac{1}{a^\gamma} P(x/a^\gamma, \tau) \right] dx = 0 \quad (\text{A5})$$

for all  $a > 0$  and for all  $x_0$ . From the continuity of the function  $P(x, \tau)$ , a simple continuity argument yields equation (2). The argument is as follows. It follows from the previous equation that

$$\int_{\alpha}^{\beta} \left[ P(x, a\tau) - \frac{1}{a^\gamma} P(x/a^\gamma, \tau) \right] dx = 0 \quad (\text{A6})$$

for any  $\alpha$  and  $\beta$ . Suppose that there exists a point  $x_0$  and  $a > 0$  such that the integrand is nonzero at the point  $x_0$ . Also suppose that the integrand is positive when evaluated at the point  $x_0$ . Then, by the continuity of  $P(x, t)$ , there exists  $\alpha$  and  $\beta$  such that the integrand is positive throughout the interval  $\alpha < x_0 < \beta$ . Thus

$$\int_{\alpha}^{\beta} \left[ P(x, a\tau) - \frac{1}{a^\gamma} P(x/a^\gamma, \tau) \right] dx > 0, \quad (\text{A7})$$

a contradiction. Hence the integrand is zero for all  $x$ .

[35] **Acknowledgments.** J.J.P. would like to thank Leonard F. Burlaga and Adolfo Viñas for bringing to his attention the papers by Hnat et al. Special thanks are due to Ronald Lepping for comments on the initial manuscript and to the referee whose helpful comments led to an improved presentation of the results. The spacecraft data used in this study was provided by the Space Physics Data Facility at Goddard Space Flight Center.

[36] Amitava Bhattacharjee would like to thank the reviewers for their assistance in evaluating this paper.

## References

- Baroud, C. N., and H. L. Swinney (2003), Nonextensivity in turbulence in rotating two-dimensional and three-dimensional flows, *Physica D*, *184*, 21.
- Baroud, C. N., B. B. Plapp, Z.-S. She, and H. L. Swinney (2002), Anomalous self-similarity in a turbulent rapidly rotating fluid, *Phys. Rev. Lett.*, *88*, 114501.
- Baroud, C. N., B. B. Plapp, H. L. Swinney, and Z.-S. She (2003), Scaling in three-dimensional and quasi-two-dimensional rotating turbulent flows, *Phys. Fluids*, *15*, 2091.
- Embrechts, P., and M. Maejima (2002), *Selfsimilar Processes*, Princeton Univ. Press, Princeton, N. J.
- Hnat, B., S. C. Chapman, G. Rowlands, N. W. Watkins, and W. M. Farrell (2002), Finite size scaling in the solar wind magnetic field energy density as seen by WIND, *Geophys. Res. Lett.*, *29*(10), 1446, doi:10.1029/2001GL014587.
- Hnat, B., S. C. Chapman, and G. Rowlands (2003), Intermittency, scaling, and the Fokker-Planck approach to fluctuations of the solar wind bulk plasma parameters as seen by the WIND spacecraft, *Phys. Rev. E.*, *67*, 056404.
- Lepping, R. P., et al. (1995), The WIND magnetic field investigation, *Space Sci. Rev.*, *71*, 207.
- Mangency, A., C. Salem, P. L. Veltri, and B. Cecconi (2001), Intermittency in the solar wind turbulence and the Haar wavelet transform, Proceedings of the Les Woolliscroft Memorial Conference, *Eur. Space Agency Spec. Publ.*, *ESA-SP-492*, 53.
- Samorodnitsky, G., and M. S. Taqqu (1994), *Stable Non-Gaussian Random Processes*, CRC Press, Boca Raton, Fla.
- Smith, C. W., M. H. Acuna, L. F. Burlaga, J. L'Heureux, N. F. Ness, and J. Scheifele (1998), The ACE magnetic fields experiment, *Space Sci. Rev.*, *86*, 613.
- Tanskanen, E. I., J. A. Slavin, A. J. Tanskanen, A. Viljanen, T. I. Pulkkinen, H. E. J. Koskinen, A. Pulkkinen, and J. Eastwood (2005), Magnetospheric substorms are strongly modulated by interplanetary high-speed streams, *Geophys. Res. Lett.*, *32*, L16104, doi:10.1029/2005GL023318.
- Veltri, P., and A. Mangency (1999), Scaling laws and intermittent structures in solar wind MHD turbulence, in *Solar Wind Nine*, edited by S. R. Habbal et al., *AIP Conf. Proc.*, *471*, 543.
- Zachmanoglou, E. C., and D. W. Thoe (1986), *Introduction to Partial Differential Equations With Applications*, Dover, Mineola, N. Y.

---

M. L. Goldstein, J. J. Podesta, and D. A. Roberts, Laboratory for Solar and Space Physics, NASA Goddard Space Flight Center, Code 612.2, Greenbelt, MD 20771, USA. (jpodesta@solar.stanford.edu)